

Characteristics of second-harmonic generation in HeXLN

Martijn de Sterke

School of Physics, University of Sydney, NSW 2006, Australia

N.G.R. Broderick, T.M. Monro and David J. Richardson

Optoelectronics Research Centre, Univ. of Southampton, Southampton, SO17 1BJ, UK

Abstract– We study second harmonic generation in hexagonally poled LiNbO₃. We model this process theoretically assuming an undepleted pump, and use the Fraunhofer approximation to determine the required optical path lengths. The results of this procedure are in good agreement with experiments.

Introduction

Periodic poled LiNbO₃, in which the sign of the quadratic nonlinear coefficient $\chi^{(2)}$ varies periodically in one direction, is a well-established geometry to achieve quasi-phase matching in frequency conversion processes such as second-harmonic generation (SHG) [1]. Indeed, very high conversion efficiencies have been reached in these structures. This can be understood as the contribution of a reciprocal lattice vector of the periodic structure to the phasematching process. Hexagonally poled LiNbO₃ (HeXLN), originally proposed by Berger in 1998 [2], constitutes a generalization in that the $\chi^{(2)}$ coefficients varies according to a hexagonal lattice; it is thus periodic in two directions, rather than in a single one. The much richer reciprocal lattice of two-dimensional lattices allows for a larger variety frequency conversion processes to occur in a single structure.

The fabrication of a HeXLN crystal was recently reported by Broderick *et al* [3]. Using a fiber laser pump source emitting around $\lambda = 1530$ nm, simultaneous second, third and even fourth harmonic generation was reported in this structure. [3] Here we analyze the characteristics of the SHG process theoretically, and compare with experimental results.

Description of the process

A schematic of a HeXLN crystal is shown in Figure 1(a). The sign of $\chi^{(2)}$ in the shaded regions is inverted with respect to that in the clear regions. Note that the inverted regions form a hexagonal lattice and that each inverted region has an hexagonal shape. The fundamental frequency (FF) light travels in the horizontal (K) direction. The insert shows the Brillouin zone of the hexagonal lattice with various points of high symmetry. Figure 1(b) shows how (quasi-) phasematching, which requires

$$2\mathbf{k}_f - \mathbf{k}_s = \mathbf{G}, \quad (1)$$

where \mathbf{k}_f and \mathbf{k}_s are the FF and second harmonic (SH) wavevectors, respectively, and \mathbf{G} is the relevant reciprocal lattice vector, is achieved.

In the experiments we consider here, the FF is a Gaussian beam with a full-width at half-maximum of $150 \mu\text{m}$, traveling through 10 mm of HeXLN. Input powers are sufficiently low for the undepleted pump approximation to apply. Taking the relevant refractive indices for LiNbO₃ [4] it is found that at a temperature of $T = 150^\circ$ Celsius, phase matching occurs at $\lambda_f = 1.531 \mu\text{m}$, and the SH propagates at an angle $\vartheta_i = 0.640^\circ$ with respect to the FF within the LiNbO₃, corresponding, via Snell's law, to an external angle of $\vartheta_o = 1.40^\circ$, in good agreement with experiments.

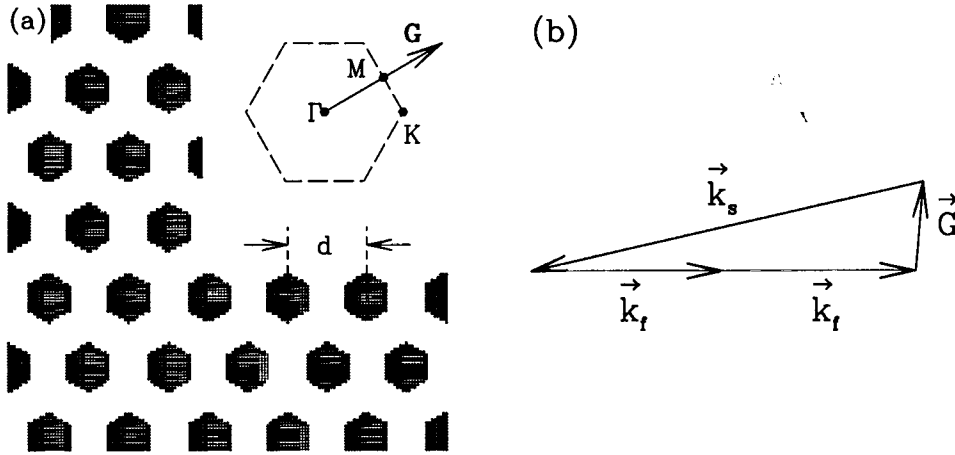


Figure 1: (a) Schematic of a HeXLN crystal with period of $d = 18.05 \mu\text{m}$. The inset shows the hexagonal lattice's Brillouin zone (dashed line). Phase matching is achieved using the reciprocal lattice vector \mathbf{G} . (b) Indicates the phasematching in real space; for clarity, the vertical scale has been expanded by a factor 20.

Theory and results

In the usual way to model frequency conversion processes, the propagation directions of the various frequencies are prescribed from the outset. This assumes that the relevant reciprocal lattice vector is known *a priori* [6]. Here, however, in spite of Figure 1(b), there was initially some uncertainty about this vector [3]. We have therefore adopted a Green function method in which all reciprocal lattice vectors have the same status, and none is preferred [5]. In this method, the nonlinear polarization \mathbf{P}_{NL} at each position \mathbf{r} is calculated in the undepleted pump approximation. The electric field at the second harmonic frequency at an observation point \mathbf{r}' is then

$$\mathbf{E}(\mathbf{r}') \propto \int d\mathbf{r} G(\mathbf{r}; \mathbf{r}') \mathbf{P}_{NL}(\mathbf{r}), \quad (2)$$

where the $G(\mathbf{r}; \mathbf{r}')$ is the Green function of the two-dimensional Helmholtz equation

$$G(\mathbf{r}; \mathbf{r}') = \frac{H_0^{(1)}(k_s |\mathbf{r} - \mathbf{r}'|)}{4i}, \quad (3)$$

where $H_0^{(1)}$ is the zeroth order Hankel function of the first kind. The implementation of Eqs. (2) and (3) is straightforward: since the observation point is about 40 cm from the sample, it is very well justified to use the asymptotic expansion of the Hankel function for large arguments. This also allows one to approximate the path difference $|\mathbf{r} - \mathbf{r}'|$ using the Fraunhofer approximation.

Results of such a calculation are shown in Figs 2. Fig. 2(a) is a contour plot of the SH generation efficiency at a fixed fundamental wavelength of $\lambda = 1.5290 \mu\text{m}$, versus temperature and external angle. Note that at a fixed angle, the efficiency has the standard sinc^2 behavior, but that the peak of this function varies with angle, resulting in the skew in Fig. 2(a). Experimental measurements of the SH efficiency are not angle-resolved, and thus correspond to averaging over angle. The result of this is given by the solid line in Fig. 2(b), and the corresponding measurement, taken at 50 mW pump power, is indicated

by the dashed line. The two results are clearly in good agreement. Note that the two curves do not exhibit usual prominent side lobes. This can be understood from the skew of the contours in Fig. 2(a). Many of the features in Fig. 2(a) can be understood analytically. For example, for the small propagation angles of $1^\circ - 2^\circ$ in the experiment, the skew direction in Fig. 2 is given by

$$\frac{d\vartheta_o}{dT} = \frac{k'_f - (k'_s/2) \cos(\vartheta_i)}{k_s \sin(\vartheta_i)} \quad (4)$$

where $k'_f = dk_f/dT$, and similarly for k'_s . Similar results, both experimentally and theoretically, have been obtained at fixed temperature, as a function of wavelength. The results are in similarly good agreement with each other.

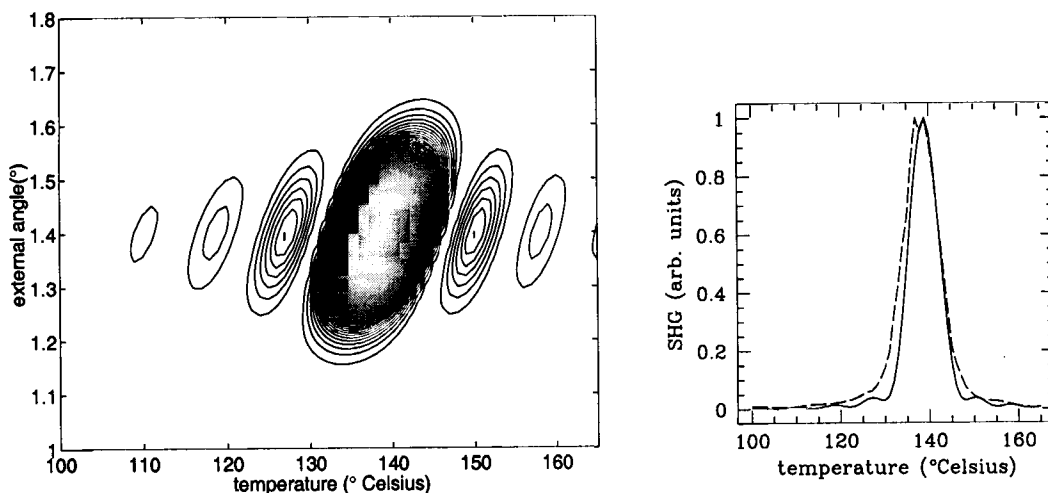


Figure 2: (a) SH generation efficiency as functions of temperature and external angle ϑ_o at the fixed FF wavelength of $\lambda = 1.5290 \mu\text{m}$. (b) Dashed line: experimental result for SH efficiency versus temperature; solid line: results in (a) integrated over angle.

Discussion and conclusion

Though it is clear that the basic properties of SHG in HeXLN are well understood, many other issues remain, which cannot necessarily be solved in the straightforward way discussed here. These include lattice imperfections, the effects of scattering off linear refractive index variations, third- and higher harmonic generation, high pump powers where the undepleted pump approximation is not valid, etc. These will be the subject of future study.

MdS acknowledges support from the Australian Research Council.

References

- [1] M.M. Fejer, G.A. Magel, D.H. Jundt, and R.L. Byer, *J. Quantum Electron.* **28**, 2631 (1992).
- [2] V. Berger, *Phys. Rev. Lett.* **81**, 4136 (1998).
- [3] N.G.R. Broderick, G.W. Ross, H.L. Offerhaus, D.J. Richardson, and D.C. Hanna, *Phys. Rev. Lett.* **84**, 4345 (2000).
- [4] D.H. Jundt, *Opt. Lett.* **22**, 1553 (1997).
- [5] M.J. Steel and C.M. de Sterke, *Appl. Opt.* **35**, 3211 (1996).
- [6] R.W. Boyd, *Nonlinear optics* (Academic, San Diego, 1992).